[17] R. C. Franz, R. J. Nemzek, and J. R. Winckler, "Television image of a large upward electrical discharge above a thunderstorm system," *Science,* vol. 249, p. 48, 1990.
[18] Y. N. Taranenko, U. S. Inan, and T. F. Bell, "Optical signatures of lightning-induced heating of the D-region," *Geophys. Res. Lett.,* vol. 19, p. 1815, 1992.
[19] M. C. Kelley, J. G. Ding, and R. H. Holzworth, "Intense electric and magnetic field pulses generated by lightning," *Geophys. Res. Lett.,* vol. 17, p. 2221, 1990.
[20] Y. Q. Li, R. H. Holzworth, H. Hu, M. McCarthy, D. Massey, P. M. Kintner, J. Rodriguez, U. S. Inan, and W. C. Armstrong, "Anomalous optical events detected by rocket- and balloon-mounted detectors in the WIPP campaign," *J. Geophys. Res.,* vol. 96, p. 1315, 1991.
[21] F. Hepburn, "Atmospheric waveforms with very low-frequency components below 1 kc/s known as slow tails," *J. Atmos. Terr. Phys.,* vol. 10, p. 266, 1957.
[22] Z. Ma, Ph.D. thesis, Penn State University, 1995.
[23] R. A. Roussel Dupré, A. V. Gurevich, A. V. Tunnell, and G. M. Milikh, "Kinetic theory of runaway air breakdown," *Phys. Rev.,* vol. E 49, no. 3, p. 2257, 1994.
[24] T. F. Bell, V. Pasko, and U. Inan, "Runaway electrons as a source of red sprites in the mesosphere," *Geophys. Res. Lett.,* vol. 22, p. 2127, 1995.

Genetic Algorithm Design of Pareto Optimal Broadband Microwave Absorbers

D. S. Weile, E. Michielssen, and D. E. Goldberg

Abstract— **The concept of Pareto optimality is applied to the study of choice tradeoffs between reflectivity and thickness in the design of multilayer microwave absorbers. Absorbers composed of a given number of layers of absorbing materials selected from a predefined database of available materials are considered. Three types of Pareto genetic algorithms for absorber synthesis are introduced and compared to each other, as well as to methods operating with the weighted Tchebycheff method for Pareto optimization. The Pareto genetic algorithms are applied to construct Pareto fronts for microwave absorbers with five layers of materials selected from a representative database of available materials in the 0.2–2 GHz, 2–8 GHz, and 9–11 GHz bands.**

I. Introduction

Multilayer microwave absorptive coatings are often used in concert with other devices for reducing the radar cross section of a wide diversity of objects, and they find use in variegated applications ranging from stealth to anechoic chambers. In general, such coatings must not only suppress reflection over a wide band of frequencies, but also need to be thin to be practical and economical. These two goals—thinness and low reflectivity—very often conflict, and designers are forced to rely upon experience or prolonged experiments

Manuscript received September 22, 1995; revised April 22, 1996. This work was funded in part by the University of Illinois Research Board and the National Science Foundation under Grant ECS-9502138. D. E. Goldberg's effort was sponsored by the Air Force Office of Scientific Research, Air Force Materiel Command, USAF, under Grants F49620-95-1-0338 and F49620-94-1-0103.

D. S. Weile and E. Michielssen are with the Electromagnetic Communication Laboratory, University of Illinois at Urbana-Champaign, Urbana, IL 61801 USA.

D. E. Goldberg is with the Illinois Genetic Algorithms Laboratory (IlliGAL), University of Illinois at Urbana-Champaign, Urbana, IL 61801 USA.

Publisher Item Identifier S 0018-9375(96)06349-1.

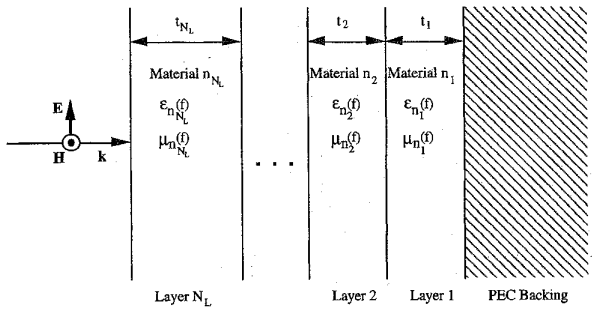

Fig. 1. Multilayer absorptive coating under investigation. The GA can chose the t's (up to 2 mm) and the n's (from Table I) to find a good tradeoff.

to determine what tradeoffs are feasible within prescribed design constraints. In cases where thinness and absorption do conflict, the "optimal" design with respect to high absorption may be too thick or expensive to be practical. An engineer is therefore often interested in the thinnest absorber he can build with a given level of reflection suppression. Such designs are known in the optimization literature as *Pareto optimal*, as they share the quality that no design in the search space is simultaneously thinner and less reflective [1]–[3]. The set of designs which are thinnest for a every achievable level of reflectivity forms a manifold known as the *Pareto front.* In this paper, we present a technique for the design of multilayered broadband microwave absorbers (Fig. 1) which given:

- a database of available materials with arbitrarily frequency dependent properties;
- a number of incident angles where reflection is to be suppressed;
- a number of frequencies across a band over which the absorber is to operate

obtains a discrete approximation to the Pareto front of absorbers with a fixed number of layers describing optimal tradeoffs between thickness and some norm of the reflections at all of the given frequencies and angles of interest. *While no algorithm can be guaranteed to find the absolute Pareto front for arbitrary problems,* knowledge of the Pareto front would provide the designer of microwave absorbers all optimal alternatives: Designs represented by points on the Pareto front reflect as little as possible for a given thinness of coating; designs represented by points not on the front are either physically unrealizable within the constraints of the problem, or represent an inferior tradeoff to a design on the curve [Fig. 2(a)].

Historically, a number of studies on the topic of microwave absorbers have been undertaken using several different schemes. The vast majority of these studies (e.g., [4]–[8]) use either approximate closed-form analytic expressions or steepest descent optimization methods; alternative techniques based on optimal control methods have also been proposed [9]. Most recently, Perini and Cohen suggested [10] a technique based on the modified Powell algorithm which does not rely on any explicit gradient information. Since all of these classical optimization algorithms process information about the local characteristics of the function, they by nature find local optima near the starting point of the algorithm. If the search space is quite multimodal, many of these techniques may need to be restarted several times to arrive at an acceptable optimum. Indeed, Pesque *et al.* [9] recommend that their optimal control technique be supplemented by simulated annealing to overcome the local optimum trap. Also, because most of these methods optimize material

0018–9375/96$05.00 © 1996 IEEE

parameters, the design the algorithm generates may be physically unrealizable, forcing the designer to pick existing materials similar to those found by the search, and reoptimize the thicknesses [10]. Finally, as none of these methods manipulate more than one design to search for optima, they can not return a Pareto optimal set of designs without laborious iteration.

Genetic Algorithms (GA's) have been applied to the design of microwave absorbers [11]–[13] as well as to the design of such multifarious devices as optical filters, antenna arrays, and broadband loaded wire antennas [14]–[18]. GA's are nonlinear, stochastic algorithms based loosely upon the Darwinian theory of descent with modification by natural selection [19], [20]. Though absolute convergence of the algorithm is not guaranteed, and the convergence of GA's is much slower than local searches, the stochastic nature of GA's makes them less likely to converge to weak local optima [19]. In addition, GA's typically operate on binary encodings of the search variables. In the present study this implies that the GA can draw from a database of available materials with arbitrary characteristics, ensuring that the design found by the algorithm can be realized.

All of the GA studies mentioned above [11]–[18] use GA's for single objective optimization. In this paper, we describe and compare several Pareto GA schemes which construct approximations to the Pareto front for the absorber design problem outlined above. Pareto GA's are GA's augmented with specialized operators to permit multiobjective optimization, for which GA's are ideally suited since they are population-based.

This paper is organized as follows. Section II describes the specific problem under consideration and the operation of Pareto GA's. Section III relates the results obtained using various implementations of the Pareto GA for several practical design problems. Section IV presents the conclusions of this study.

II. Formulation

In this section we describe a number of techniques for designing Pareto optimal stratified absorbers using GA's. Section II-A describes techniques for analysis of layered microwave absorbers and defines the concept of Pareto optimality with applications to the problem at hand. Section II-B reviews standard GA's geared toward single objective optimization with special emphasis on the specific genetic operators that find use in this study. Section II-C discusses several additional techniques that allow the standard GA to accomplish mulitobjective optimization without iteration of a single objective GA. Lastly, Section II-D discusses several practical implementations of Pareto GA's using different combinations of the techniques introduced in Sections II-B and II-C.

A. Design of Pareto Optimal Microwave Absorbers

Consider a planar stratified absorber composed of N_L layers of different materials stacked on a Perfect Electric Conductor (PEC) (Fig. 1). We wish to select these materials such that they suppress reflection of an incident plane wave over a frequency band B, but remain as thin a possible. The materials for the different layers are selected from a predefined, finite database of available materials whose constitutive parameters may vary arbitrarily with frequency.

For any frequency f we may recursively evaluate the reflection coefficient, $R(f)$, of a plane wave normally incident on an absorber composed of N_L layers of thicknesses t_i, permittivities $\varepsilon_i(f)$, and permeabilities $\mu_i(f)\,(i \in \{1, 2, \cdots, N_L\})$ backed by a conductive sheet as [21]

$$R_i(f) = \frac{\tilde{R}_i(f) + R_{i-1}(f)e^{-2jk_{i-1}(f)t_{i-1}}}{1 + \tilde{R}_i(f)R_{i-1}(f)e^{-2jk_{i-1}(f)t_{i-1}}} \tag{1}$$

where

$$\tilde{R}_i(f) = \frac{\mu_{i-1}(f)k_i(f) - \mu_i(f)k_{i-1}(f)}{\mu_{i-1}(f)k_i(f) + \mu_i(f)k_{i-1}(f)} \tag{2}$$

for $i > 0$, $k_i(f) = 2\pi f\sqrt{\mu_i(f)\varepsilon_i(f)}$, $\tilde{R}_0 = -1$, and $R(f) = R_{N_L}(f)$. This process can then be repeated over a representative set of frequencies within the band B to find the frequency response of the absorber. The analysis for the more general case of multiple angles of incidence is not much different than the case of normal incidence [21] and is not presented here. The total thickness of the absorber, t, is given by

$$t = \sum_{i=1}^{N_L} t_i. \tag{3}$$

We wish to minimize both $R = 20\log_{10}\{\max[R(f)], / f \in B\}$, the highest reflection over the band, and the total thickness t. Because we seek the simultaneous minimization of two conflicting goals simultaneously, there are many possible tradeoffs that require consideration. The concept of Pareto optimality provides a framework for defining exactly what is meant by "optimal tradeoff."

Though the problem at hand only involves the minimization of two parameters, the concept of Pareto optimality (and by implication, Pareto GA's) can be applied to design problems of any number of criteria. Imagine a design problem with a vector $\mathbf{f} = (f^1, \cdots, f^G)$ of G objectives, each of which we wish to minimize, and two candidate designs with objective function vectors $\mathbf{f}_1$ and $\mathbf{f}_2$, respectively. Design 1 is said to *dominate* design 2 (or $\mathbf{f}_2$ is said to be *inferior* to $\mathbf{f}_1$) if for all $i \in \{1, 2, \cdots, G\}$ $f_1^i \leq f_2^i$, and there exists at least one i such that $f_1^i < f_2^i$. A design is said to be *nondominated* if there exists no feasible design in the entire solution space which dominates it. The Pareto front is the set of all such nondominated designs [1]–[3], [19], [22].

Once constructed, the Pareto front can be used to find the optimal design for a given absorber application. If the application requires the most absorbent design to be no thicker than a certain value $t_{\max}$, the Pareto front can be scanned in the direction of thinner designs starting with the thickest design until a design of thickness $t_{\max}$ is located. This design is the most absorbent design located by the algorithm which meets the stated specifications. Once this design is discovered, the designer can look at how much absorptivity he would need to sacrifice by going to a slightly thinner design. If a much thinner design has roughly the same absorptivity, it may be a sound engineering decision to use it instead of the design with thickness $t_{\max}$.

B. Introduction to Genetic Algorithms for Single Objective Optimization

As discussed in the introduction, this study uses GA's to find a discrete approximation of the Pareto front. GA's are a class of algorithms which can be applied to reliably find strong local or global optima of a function over a given domain of interest. Loosely based on the principle of survival of the fittest, GA's are complicated like Nature herself: They are nonlinear, stochastic, and highly parallel in structure [19], [20].

Unlike more standard classical optimization algorithms, GA's do not operate on single design candidates, but simultaneously act on a whole population of N_p designs. The designs are represented in the population by encoding salient design parameters into bit strings of length N_b called *chromosomes,* after which an initial population of N_p candidate designs is created at random. The GA operates by repeated application of genetic operators to entire populations resulting in a succession of populations of improved designs. For the

specific problem considered in this paper, chromosomes are encoded as follows. The chromosome for an N_L layer design consists of $2N_L$ *genes.* Half of these genes are composed of N_m bits and decode to an integer identifying the material choice for a given layer in the database; the other half contain N_t bits and decode via a linear transformation to the thickness of a layer [12]. Thus, each chromosome is composed of $N_b = N_L \times (N_m + N_t)$ bits. Though the GA literature abounds with examples of different operators to improve the GA's ability to search this prodigious expanse of design possibilities, all GA's include three basic operators: *selection, crossover, and mutation* [19], [20].

The selection operator implements the principle of survival of the fittest, and by so doing is the primary operator responsible for convergence of the algorithm [19], [20]. All designs in the population are evaluated according to an *objective function F* which measures the quality of a solution to a given problem, and represents the quantity optimized by the GA. Selection creates a new generation of N_p designs by allotting more positions in the new population to those designs with favorable objective function values, and eliminating those with poor values. Though there exist several schemes in the literature for accomplishing this, this study uses only the two most common: *tournament selection* in which the better of two randomly chosen designs in placed into the new population until the population is full, and *roulette-wheel selection* which fills each spot in the new population by selecting designs out of the old population with probability proportional to their fitness.

Once selection has produced a new population of size N_p, the crossover operator constructs another new population of size N_p by combining information from successful designs. Chromosome pairs are picked at random from the population and are crossed over with some predetermined probability p_c usually between 0.8 and 1. For each pair that is to be crossed over, a random crossover site is picked between the kth and $k+1$th bits of the pair. The selected chromosomes then exchange their $k+1$th through lth bits yielding children chromosomes. Chromosome pairs not chosen for crossover are copied unmodified into the next generation [19], [20].

Finally, the mutation operator is applied to prevent premature convergence of the GA, by performing a logical NOT on a few bits in the population randomly selected with probability $0.0005 < p_m < 0.01$. Mutation is not the primary search instrument of the GA but is included mainly to prevent the loss of information, initially contained in chromosomes that die off prematurely, but which contain information which may prove useful to the GA in later generations [19], [20].

Selection, crossover, and mutation are repeatedly applied to successive populations until some termination criterion is satisfied. Usually, the GA is stopped either when it meets some preset design goal, when a predetermined number or generations has passed, or when no substantial improvement in the objective function value is observed.

When a single objective GA (such as described above) is successfully applied to absorber design via a linear combination of objectives $F = R + \alpha t$ as in [12], all population members converge to a single point on the Pareto front [Fig 2(b)]. We might attempt to construct the Pareto front by iterating the GA for various values of α. In fact, a comparison between the designs found in [12] and this study shows those designs to indeed be a subset of the designs found here. Unfortunately, this *weighting method* is doomed to failure as it is clear from Fig. 2(b) that it will be incapable of finding concave portions of the curve [1]–[3]. A better approach is to use the *weighted Tchebycheff procedure,* which involves minimizing the objective function [3], [23]

$$F = \max\left[\alpha t,\ \sqrt{1-\alpha^2}(R - R^M)\right] \tag{4}$$

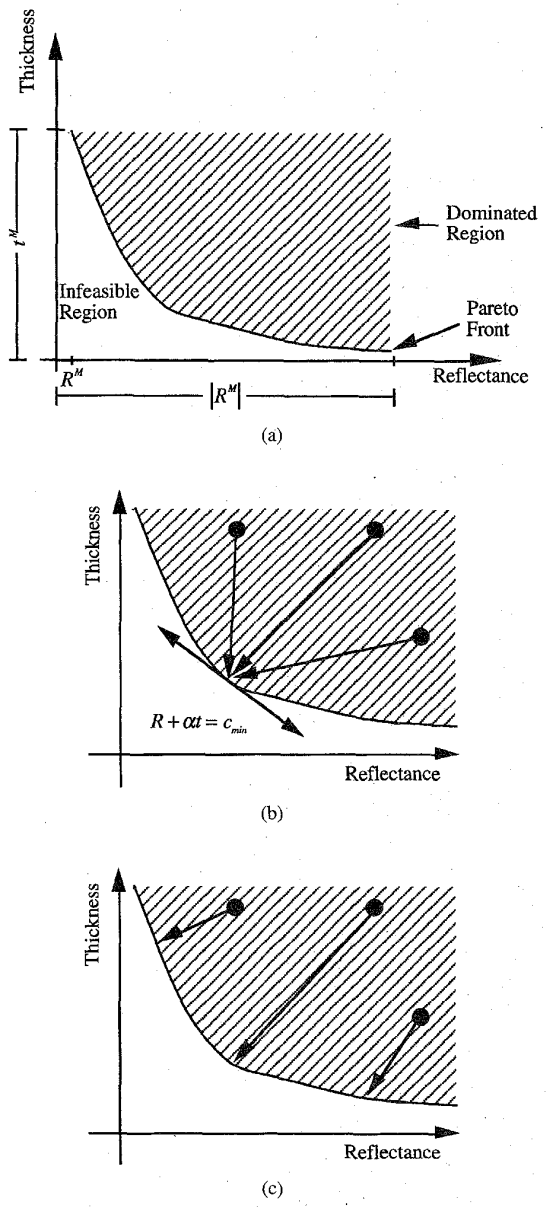

Fig. 2. (a) A typical Pareto front. Anything in the hashed region represents an inferior design as there is a design on the front that is more absorptive for the same thickness, any design in the white region is physically unrealizable. (b) Convergence of standard GA. (c) Desired convergence of Pareto GA.

for values of α ranging from 0 to 1 and where R^M is an ideal value for the reflectivity in decibels. While this function is capable of generating concave parts of the Pareto front, the process of iterating it for many values of α is computationally wasteful (see Section III), and does not capitalize on the greatest asset of the GA: the wealth of information contained in its population. Thus, we want the behavior of the GA to be like that of Fig. 2(c), where the population spreads out uniformly over the front.

C. Alterations to the Standard GA for Pareto Genetic Algorithms

Several advanced operators have to be added to the single objective GA if the Pareto front is to be located in only one run. These operators assist the GA in pushing the population to the edge of the

feasible region, and to ensure the designs spread evenly and densely on the front. Since a Pareto GA must return a curve dense enough to accurately represent the Pareto front and diverse enough to present the full range of possible designs, these operators are essential to the proper behavior of the GA.

A design evaluated according to multiple objectives is considered Pareto optimal if it is nondominated—that is, if there exists no feasible design which is simultaneously superior with respect to all objectives. The definition of Pareto optimality therefore imposes two separate (but intimately related) challenges to the traditional GA: Pareto GA's must: i) select designs on the basis of their relative Pareto dominance standing in the population, and ii) force the population to converge to a diverse Pareto front, not a single design. If diversity is not actively encouraged in the GA, chromosomes in the population tend to unevenly distribute themselves along the Pareto front resulting in instability known as *genetic drift.* Since the GA is more likely to promulgate traits of the most prevalent designs in a given population, these designs garner more representatives in the population which may result in the loss of diversity. Any successful Pareto GA must both capably evaluate the dominance relations in the population, as well as maintain diversity for the length of the GA run.

Besides Schaffer's initial attempts at Pareto optimization [24], [25], all other Pareto GA's proposed in the literature [22], [26], [27] are variations of a suggestion from Goldberg [19] that the twin problems of Pareto GA's be handled separately. To select designs according to Pareto dominance, Goldberg suggests the use of *nondomination ranking.* Specifically, Goldberg delineates a scheme where all nondominated population members are assigned a rank of one and removed from the population. The nondominated members in the remaining part of the population are then assigned a rank of two, and so on, until the entire population is ranked. Each design then receives a fitness based on its nondomination ranking.

To prevent the effects of genetic drift, Goldberg suggests the use of *niching* methods, which were originally developed so that GA's could converge to more than one peak in multimodal problems, but since have been applied to general GA search and Pareto GA's as well [19], [28]. The oldest niching method, called *crowding,* was introduced in DeJong's thesis [28]. Crowding preserves niches by preferentially eliminating over-represented designs so that, when new designs are placed in the population, novel designs in the current generation have a higher probability of survival than hackneyed ones [19], [28]. A complete description of the crowding algorithm may be found in [19].

Another method for maintaining diversity in the population is *fitness sharing* [19], [29]. Fitness sharing is based on Malthusian competition between organizms for limited resources in relation to the preservation of species under natural selection. In a fitness sharing GA, besides calculating the objective function value F_i for each chromosome i, the GA calculates a *niche count* m_i which measures the density of the population surrounding that chromosome. The niche count is calculated according to the formula

$$m_i = \sum_{j=1}^{N_p} Sh(d_{i,j}) \tag{5}$$

where $Sh(d)$ is a monotonically decreasing function of x such that $Sh(0) = 1$, and $d_{i,j}$ is a distance measure between designs i and j. In this study, we use the *triangular sharing function*

$$Sh(d) = \begin{cases} 1 - \dfrac{d}{\sigma_{share}} & d < \sigma_{share} \\ 0 & d \geq \sigma_{share} \end{cases} \tag{6}$$

where σ_{share} is a designer chosen *niche radius.* This study uses *phenotypic sharing,* i.e., we measure distances between design properties rather than the Hamming distance between the chromosomes describing a design. Phenotypic sharing may be performed on either: i) the design parameters as *decoded* from the chromosome (here the layer thicknesses and material choices) or ii) the chromosome's objective function vector (R, t). In Pareto GA's, type ii) phenotypic sharing is usually preferred because we seek a large variety of different optimal tradeoffs in *objective function* space, but we care little whether or not different points on the Pareto front represent large differences in the design of the absorber itself [22], [27]. All objectives are effectively scaled to range between 0 and 1 to ensure that the metric weighs objectives equitably [22], [26], [27].

Once the m_i have been calculated, chromosomes are reproduced assuming an objective function value of $F_{shared,i} = F_i/m_i$ instead of F_i so that the GA will not allow all chromosomes to converge to one solution, but will try to achieve a steady state where any two chromosomes i and j in the population will satisfy [19], [29]

$$\begin{aligned} F_{shared,i} &= \frac{F_i}{m_i} \\ &= \frac{F_j}{m_j} \\ &= F_{shared,j}. \end{aligned} \tag{7}$$

In Pareto GA's, sharing is used to get a better representation of the front since at equilibrium, all nondominated designs will need to spread along the front out or die off. Lastly, we note that the entire population need not be used to calculate the niche counts m_i; simply sampling some percentage of the population to estimate the niche count usually suffices.

D. Implementations of the Pareto Genetic Algorithm

This section details three specific implementations of the Pareto GA. The first implementation uses the nondomination ranking scheme described in Section II-C with crowding and tournament selection. We refer to this as the Crowded Tournament Pareto GA (CTPGA).

The second Pareto GA used is known as the Niched Pareto GA (NPGA) [27]. Instead of explicitly using nondomination ranking, the NPGA uses *Pareto domination tournaments* which compare two randomly chosen designs to a randomly chosen comparison set of t_{dom} designs to determine their relative optimality. If no determination can be reached, the winner is chosen to be the design with less similarity to the designs already chosen for the next generation. A full description of the algorithms used can be found in [27] and [30].

Lastly, we implement a third scheme known as the Nondominated Sorting GA (NSGA) [26], which executes Goldberg's suggestions most faithfully. In the NSGA, designs are ranked using the nondomination ranking of Section II-C. The designs ranked one are given a nominal fitness value F_{R1} and then their niche counts m_i are calculated. Their shared fitness is then calculated in the usual way $F_{shared,i} = F_i/m_i$. The designs ranked two are then assigned a nominal fitness value F_{R2} less than the lowest shared objective function value of those ranked one, and then undergo sharing themselves. This process is continued until all members of the population are assigned a fitness value, and then roulette wheel selection is used to create the next population. In our implementation of the NSGA, the nominal fitness value of groups ranked less than one was actually chosen to be equal to the lowest shared fitness value of the previous group. This choice of nominal fitness value assignment tempers the quick selective action of the NSGA and helps allow the GA to maintain diversity in the population. Additionally, Srinivas and Deb use type i) phenotypic sharing in the NSGA; we, however, use type ii) because as mentioned in Section II-C we desire great

TABLE I

Lossless Dielectric Materials (μ_r=1.+j0.)		
#	ε_r	
1	10+j0.	
2	50+j0.	
Lossy Magnetic Materials (ε_r=15.+j0.) $\mu = \mu_r - j\mu_i \quad \mu_r(f) = \frac{\mu_r(1\text{ GHz})}{f^\alpha} \quad \mu_i(f) = \frac{\mu_i(1\text{ GHz})}{f^\beta}$		
#	μ_r(1 GHz),α	μ_i(1 GHz),β
3	5.,0.974	10., 0.961
4	3., 1.000	15., 0.957
5	7., 1.000	12., 1.000
Lossy Dielectric Materials (μ_r=1.+j0.) $\varepsilon = \varepsilon_r - j\varepsilon_i \quad \varepsilon_r(f) = \frac{\varepsilon_r(1\text{ GHz})}{f^\alpha} \quad \varepsilon_i(f) = \frac{\varepsilon_i(1\text{ GHz})}{f^\beta}$		
#	ε_r(1 GHz),α	ε_i(1 GHz),β
6	5., 0.861	8., 0.569
7	8., 0.778	10.,0.682
8	10., 0.778	6., 0.861
Relaxation-type Magnetic Materials $\mu = \mu_r - j\mu_i \quad \mu_r = \frac{\mu_m f_m^2}{f^2 + f_m^2} \quad \mu_i = \frac{\mu_m f_m f}{f^2 + f_m^2}$ (f and f_m in GHz) $\varepsilon_r = 15 + j0$		
#	μ_m	f_m
9	35.	0.8
10	35.	0.5
11	30.	1.0
12	18.	0.5
13	20.	1.5
14	30.	2.5
15	30.	2.0
16	25.	3.5

variety in the behavior of the multilayer, but not necessarily in its physical construction.

III. Numerical Results

In this section, we present the results of applying the aforementioned Pareto GA algorithms as well as weighted Tchebycheff algorithms to find Pareto optimal absorber designs. We design absorbers for operation over the bands from 0.2–2 GHz, 2–8 GHz, and 9–11 GHz, and compare the results obtained on the basis of both the diversity and density of the front. The database of materials used (reproduced as Table I) is from Michielssen *et al.* [12] and contains 16 materials ($N_m = 4$). For all Pareto GA's (unless otherwise stated), we set $p_c = 0.9$, $p_m = 0.005$, $N_p = 8000$, and run for 150 generations. The choices for the crossover and mutation probabilities are quite well within the ranges usually given in the GA literature, and we found that the algorithm was very robust with regard to moderate changes in them. A good rule of thumb for changing the population size is that is should be a large constant (roughly 100–1000) times the number of bits in the chromosome. In all chromosomes $N_L = 5$ (a common number of layers) and $N_t = 7$, which allows the algorithm enough precision to design a wide variety of absorbers without including too many insignificant bits.

First, all three algorithms described in Section II-D are applied to the design of absorbers in the lower frequency band of 0.2–2 GHz. Pareto fronts are shown in Fig. 3 which shows that the CTPGA with

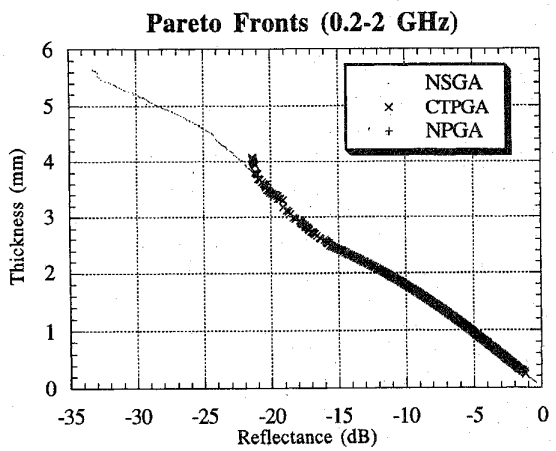

Fig. 3. The Pareto fronts obtained for the 0.2–2 GHz band.

$p_v = 0.6$ and $N_{CR} = 40$ was able to keep much diversity over the curve, as well as relatively dense front.

The NPGA, however, was unable to maintain such a compromise. Figure 3 also shows the result of running the NPGA with $t_{dom} = 100$ and a niche radius $\sigma_{share} = 0.025$ with respect to a two-dimensional phenotypic Euclidean metric defined as

$$d_{i,j} = \sqrt{\left(\frac{t_i - t_j}{t^M}\right)^2 + \left(\frac{R_i - R_j}{R^M}\right)^2}. \tag{8}$$

R^M and t^M are constants included in the metric to effectively scale both the reflectivity axis and the thickness axis to range between 0 and 1. Niche counts were estimated from sampling 2.5% of the population.

Fig. 3 shows that the best front was provided by the NSGA using the same metric and niche radius as used for the NPGA. Fig. 4 depicts the progression of the population to the front in the NSGA. Notice that by generation 10 the NSGA has located most of the Pareto front, and in the final generations the curve only becomes more well defined and just marginally more diverse. The fact that the NSGA preserves diversity through large numbers of generations is important: It implies that the designer need not check the convergence of the population every generation to ensure that diversity is not lost; he need only make sure that the GA has sufficient time to converge. We also emphasize that depending on the quality of front desired, the run time can be cut down considerably. The NSGA finds most of the front in 10 generations (80,000 objective function evaluations) and if this front is good enough, there is no need for 1.2 million it calculated in our run.

The NSGA outperforms the CTPGA and NPGA, but also is the most computationally expensive algorithm we describe, followed by the CTPGA and finally the NPGA. This is quite evident from the algorithms themselves. Both the NSGA and CTPGA involve the ranking of the entire population; the NPGA does not. Additionally, sharing is more expensive than crowding making the NSGA the most expensive algorithm of all. For the above design problem CPU time on a DEC Alpha workstation for the NSGA, the CTPGA and the NPGA were about 1 h, 50 min, and 45 min, respectively. The differences in time are not very drastic, however, because most of the computational expense comes in calculating the objective function and all three algorithms calculated it exactly the same number of times.

In addition to comparing the various Pareto GA's to each other, we present a comparison of the Pareto front obtained by the NSGA to

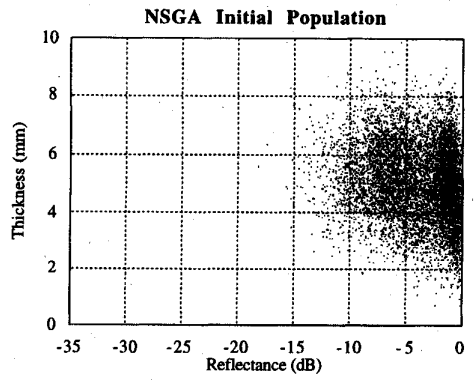

(a)

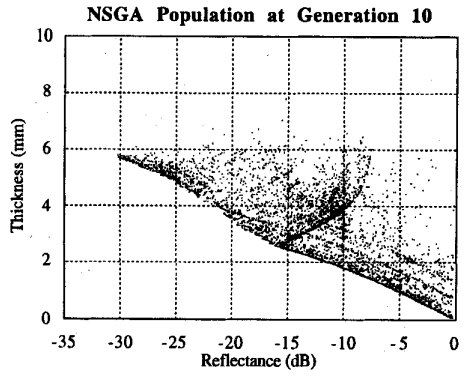

(b)

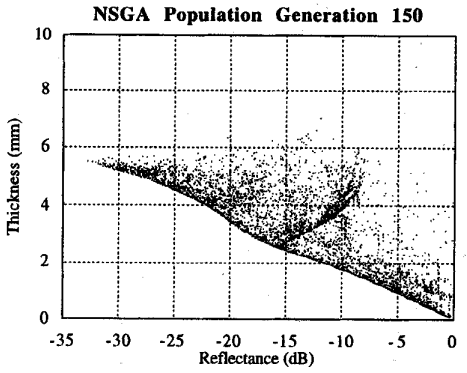

(c)

Fig. 4. The population distribution of the NSGA (a) initially, (b) in generation 10, and (c) in generation 150. Notice that the population does not change much between (b) and (c). We believe that the extra dense ridge in the population is a set of local optima; they reappear in the classical optimization schemes shown in Fig. 3.

those produced by iterated runs of Simulated Annealing (SA) and the standard GA optimizing the Tchebycheff formula (5). Like a GA, SA is a stochastic algorithm which has been applied to electromagnetic problems [9], [31], but it is based on the minimization of energy states in a Boltzmann distribution rather than the theory of evolution [32], [33]. A full description of the algorithm may be found in [33].

Since the NSGA found about 400 different points on the front, we ran both Tchebycheff schemes 400 times each with different values of α linearly spaced between 0 and 1. For the GA, we used $N_p = 100$ and ran for 100 generations to find each point, for SA we used 10 000

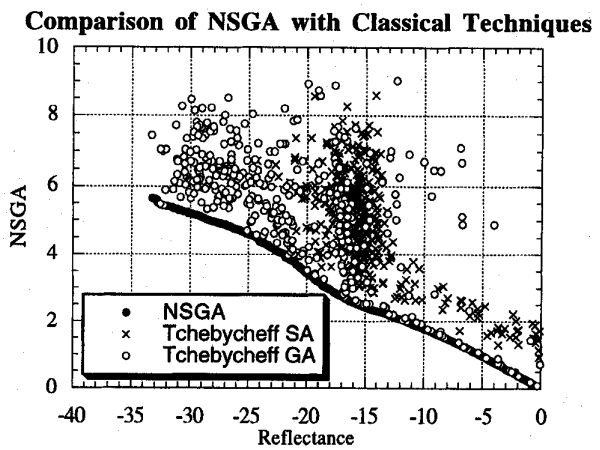

Fig. 5. The Pareto fronts obtained by "classical methods" versus the NSGA.

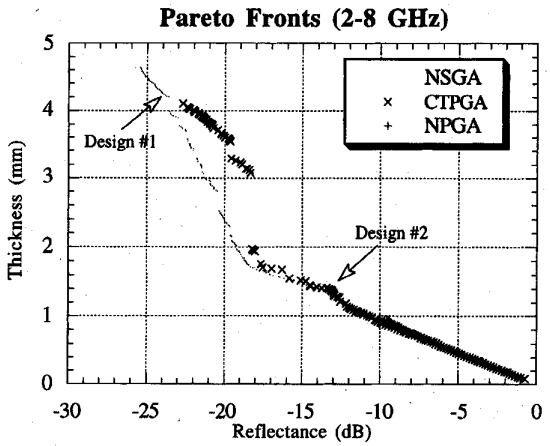

Fig. 6. The Pareto fronts obtained for the 2–8 GHz band.

iterations, giving each algorithm a total of 4 million objective function evaluations—a number more than 200% greater than the 1.2 million allotted to the NSGA and 1300% greater than the 80 000 it used to find the front of Fig. 4(b). We note that Fig. 5 demonstrates that even with the extra computational time allotted neither the standard GA nor SA could find a coherent front using the Tchebycheff formula, with many points converging to local optima rather than to the Pareto front.

We next turned to the 2–8 GHz band and found that all three Pareto GA's behaved much like in the previous example (Fig. 6). Fig. 7 and Tables II and III give the frequency response and design parameters for two particular designs on the curve. Note once again that the Pareto GA returns a whole profusion of designs in only one run. All of these designs may be stored in a database where they could easily be retrieved for future design problems with different criteria.

As a final test of the NSGA, we applied it to a problem which included multiple incidence angles as well as frequencies. The reflectivity objective function was redefined to be the highest reflection over that entire 9–11 GHz band and at incidence angles ranging from 0–70° for both TE and TM polarizations. Because of the difficulty of this problem, we took $N_p = 80000$, but only ran for 15 generations. The Pareto curve obtained by the three algorithms is shown in Fig. 8.

IV. Conclusions

This study has presented three techniques for constructing Pareto optimal designs of microwave absorbers using genetic algorithms.

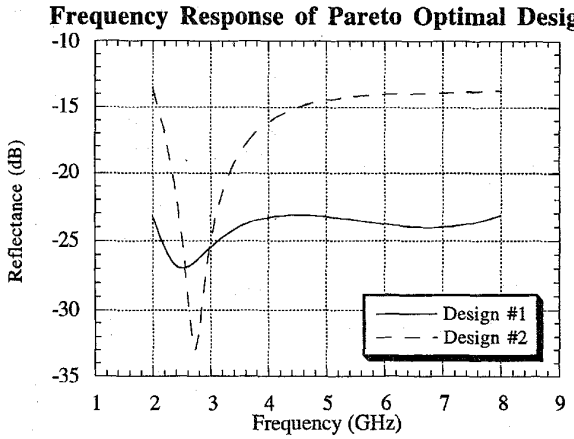

Fig. 7. The frequency responses for the two designs highlighted in Fig. 6, both of which are Pareto optimal. One design is very absorbent but quite thick, the other is more of a compromise.

TABLE II

Design #1 Parameters		
Layer Number	**Material Number**	**Thickness (mm)**
1	9	0.2506
2	15	0.5011
3	10	0.9866
4	4	1.9575
5	16	0.4385
Max. Reflectance = −23.16 dB Tot. Thickness = 4.134 mm		

TABLE III

Design #2 Parameters		
Layer Number	**Material Number**	**Thickness (mm)**
1	15	0.5481
2	8	0.4072
3	12	0.0016
4	6	0.4228
Max. Reflectance = −13.63 dB Tot. Thickness = 1.394 mm		

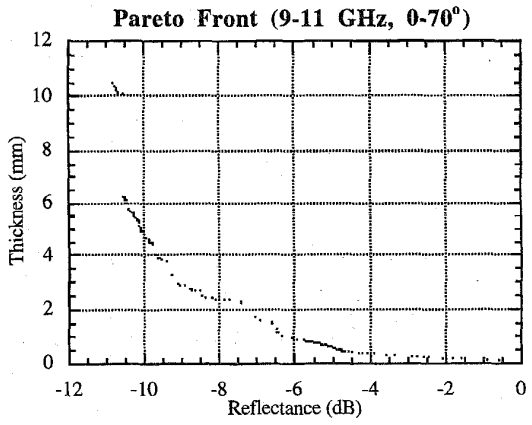

Fig. 8. The Pareto fronts for the 9–11 GHz band obtained by considering oblique incidence.

The methods employ niching techniques in combination with nondomination ranking or tournaments to present the designer of absorptive coatings with a good approximation to all of the best tradeoffs possible in only one run of the algorithm. The Pareto GA provides the designer with an abundance of optimal designs which may be applied to vastly different types of design problems. A comparison of the several Pareto GA techniques for the problem of designing absorbers was given, and results indicate that the NSGA is the algorithm most suited to this problem. The NSGA also compared favorably with both GA and SA Pareto optimization schemes based on the Tchebycheff weighing method. The technique presented may be modified to design low cost urethane cone absorbers by changing the chromosome structure and using a homogenization approach [34], [35] for the analysis. Furthermore, the materials list may be expanded to include ferrite tiles, and with the above mentioned modifications, the same algorithms could be used for the design of hybrid absorber systems [36].

ACKNOWLEDGMENT

The authors would like to thank J. Horn for his insights and knowledge of Pareto GA's.

REFERENCES

[1] J. L. Cohon, *Multiobjective Programming and Planning.* New York: Academic Press, 1978.
[2] J. L. Cohon and D. H. Marks, "A review and evaluation of multiobjective programming techniques," *Water Resources Res.*, vol. 11, no. 2, pp. 208–219, 1975.
[3] R. E. Steuer, *Multiple Criteria Optimization: Theory, Computation, Application.* Malabar, FL: Krieger, 1989.
[4] C. F. DuToit and J. H. Cloete, "Advances in design of Jaumann absorbers," in *Proc. IEEE Antennas Propagat. Soc. URSI Mtg.*, Dallas, TX, 1990, pp. 248–252.
[5] R. L. Fante and M. T. McCormack, "Reflection properties of the Salisbury screen," *IEEE Trans. Antennas Propagat.*, vol. 36, pp. 1443–1454, 1988.
[6] E. F. Knott, J. F. Schaeffer, and M. T. Tuley, *Radar Cross Section.* Dedham, MA: Artech House, 1986.
[7] H. Lidell, *Computer-Aided Techniques for the Design of Multilayer Filters.* Bristol, England: Adam Hilger, 1981.
[8] G. Ruck, D. E. Barrick, W. D. Stuart, and C. K. Krichbaum, *R.C.S. Handbook.* New York: Plenum, 1970.
[9] J. Pesque, D. Bouche, and R. Mittra, "Optimization of multilayered anti reflection coatings using an optimal control method," *IEEE Trans. Microwave Theory Technol.*, vol. 40, pp. 1789–1796, 1992.
[10] J. Perini and L. S. Cohen, "Design of broadband radar-absorbing materials for large angles of incidence," *IEEE Trans. Electromag. Compat.*, vol. 32, pp. 223–230, May 1993.
[11] B. Chambers and A. Tennant, "Design of wideband Jaumann radar absorbers with optimum oblique incidence performance," *Electron. Lett.*, vol. 30, no. 18, pp. 1530–1531, 1994.
[12] E. Michielssen, J.-M. Sajer, S. Ranjithan, and R. Mittra, "Design of lightweight, broadband microwave absorbers using genetic algorithms," *IEEE Trans. Microwave Theory Technol.*, vol. 41, pp. 1024–1031, 1993.
[13] A. Tennant and B. Chambers. "Adaptive optimization techniques for the design of microwave absorbers," in *Conf. Adaptive Computing Eng. Design Contr.*, University of Plymouth, UK, 1994, pp. 44–49.
[14] E. Michielssen, S. Ranjithan, and R. Mittra, "Optimal multilayer filter design using real coded genetic algorithms," in *IEE Proc. J*, vol. 139, 1992, pp. 413–420.
[15] S. Martin, J. Rivory, and M. Shoenauer, "Simulated Darwinian evolution of homogeneous multilayer systems: A new method for optical coatings design," *Opt. Commun.*, vol. 110, pp. 503–506, 1994.
[16] E. Michielssen, A. Boag, J. M. Sajer, and R. Mittra, "Design of electrically loaded wire antennas using massively parallel genetic algorithms," in *Proc. URSI Radio Science Mtg.*, Seattle, WA, 1994.
[17] R. L. Haupt, "Thinned arrays using genetic algorithms," *IEEE Trans. Antennas Propagat.*, vol. 42, pp. 993–999, July 1994.
[18] A. Tennant, M. M. Dawoud, and A. P. Anderson, "Array pattern nulling by element position perturbations using a genetic algorithm," *Electron. Lett.*, vol. 30, 1994.
[19] D. E. Goldberg, *Genetic Algorithms in Search, Optimization and Machine Learning.* Reading, MA: Addison-Wesley, 1989.

20] J. H. Holland, *Adaptation in Natural and Artificial Systems.* Ann Arbor, MI: University of Michigan, 1975.
21] W. C. Chew, *Waves and Fields in Inhomogeneous Media.* New York: Van Nostrand Reinhold, 1990.
22] C. M. Fonseca and P. J. Fleming. "Genetic Algorithms for multiobjective optimization: Formulation, discussion and generalization," in *Proc. Fifth Int. Conf. Genetic Algorithms,* 1993, pp. 416–423.
23] S. E. Cieniawski, J. W. Eheart, and S. Ranjithan, "Using genetic algorithms to solve a multiobjective groundwater monitoring problem," *Water Resources Res.,* vol. 31, no. 2, pp. 399–409, 1995.
24] J. D. Shaffer, "Some experiments in machine learning using vector evaluated genetic algorithms," Ph.D. dissertation, Vanderbilt University, 1984.
25] ——, "Multiple objective function optimization with vector evaluated genetic algorithms," in *Proc. First Int. Conf. Genetic Algorithms,* 1985, pp. 93–100.
26] N. Srinivas and K. Deb, "Multiobjective optimization using nondominated sorting in genetic algorithms," *Evolutionary Computat.,* vol. 2, no. 3, pp. 221–248, 1995.
27] J. Horn, N. Nafpliotis, and D. E. Goldberg. "A niched Pareto genetic algorithm for multiobjective optimization," in *Proc. First IEEE Conf. Evolutionary Computat.,* IEEE World Congress on Computational Intelligence, 1994, pp. 82–87.
28] K. A. DeJong, "An analysis of the behavior of a class of genetic adaptive systems," Ph.D. dissertation, University of Michigan, 1975.
29] D. E. Goldberg and J. J. Richardson, "Genetic algorithms with sharing for multimodal function optimization," in *Genetic Algorithms and Their Applications: Proc. Second Int. Conf. Genetic Algorithms,* 1987, pp. 41–49.
30] C. K. Oei, D. E. Goldberg, and S. J. Chang, "Tournament selection, niching, and the preservation of diversity," University of Illinois at Urbana-Champaign, 1991.
31] J. Simkin and C. W. Trobridge, "Optimizing electromagnetic devices combining direct search methods with simulated annealing," *IEEE Trans. Magnet.,* vol. 28, pp. 1343–1348, 1992.
32] S. Kirkpatrick, J. C. D. Gelatt, and M. P. Vechi, "Optimization by simulated annealing," *Science,* vol. 220, no. pp. 671–680, 1983.
33] L. Davis, *Genetic Algorithms and Simulated Annealing.* London, England: Pittman, 1987.
34] E. F. Kuester and C. L. Holloway, "A low-frequency model for wedge or pyramid absorber arrays-I: Theory," *IEEE Trans. Electromag. Compat.,* vol. 36, pp. 300–306, Nov. 1994.
35] C. L. Holloway and E. F. Kuester, "A low-frequency model for wedge or pyramid absorber arrays-II: Computed and measured results," *IEEE Trans. Electromag. Compat.,* vol. 36, pp. 307–313, Nov. 1994.
36] T. Ellam. "An update on the design and synthesis of compact absorbers for EMC chamber applications," in *Proc. 1994 IEEE Int. Symp. EMC,* Chicago, Aug. 22–26, 1994, pp. 408–412.

Predictability of Radiation in Vertical Directions Based on *In Situ* Measurements Close to the Ground at Frequencies Above 30 MHz

Ian P. Macfarlane

***Abstract*—National and international standards specify limits for the radiated disturbances created by industrial, scientific, and medical (ISM) radio-frequency equipment. The *in situ* E-field limits they specify above 30 MHz apply at heights above ground of 6 m or less. The international standard CISPR 11 specifies limits at a fixed height of 3 m. The US FCC specifies 1–4 m or 2–6 m height scans, subject to measuring distance. Specified measuring distances vary. For protection of aeronautical safety of life services, CISPR 11 specifies *in situ* limits 10 m from the exterior wall of the building housing the ISM equipment. The actual distance from the ISM equipment is not specified. This paper considers the predictability of radiation in vertical directions based on *in situ* measurements using the CISPR and FCC methods. The paper shows that the ISM fields measured by those methods are very poor guides to the fields at elevated angles. In consequence, the specified *in situ* limits cannot deliver the protection they are assumed to provide for aeronautical safety services. Recommendations are provided to improve the predictability of the fields at elevated angles.**

***Index Terms*— ISM, Numerical Electromagnetics Code (NEC), aeronautical safety of life services, vertical radiation patterns, field strength prediction.**

I. Introduction

Limits for radiated disturbances emitted *in situ* from ISM radio-frequency (RF) equipment are specified in FCC [1] and CISPR [2] standards. Above 30 MHz, the limits apply to E-fields at heights of 6 m or less. In general, the limits are to protect terrestrial radio and television services. In addition, CISPR 11 Table VI provides *in situ* limits for "protection of specific safety services." Table VI lists aeronautical services, including the instrument landing system (ILS). A note to Table VI states: "Many aeronautical communications require the limitation of vertically radiated electromagnetic disturbances. Work is continuing to determine what provisions may be necessary to provide protection for such systems."

In CISPR 11 Table VI the *in situ* measuring distance above 30 MHz is 10 m "from *(the)* exterior wall outside the building in which the equipment is situated." Significantly, *the CISPR does not specify the precise measuring distance from the ISM equipment.* The FCC specifies *in situ* measurement distances *from the ISM equipment,* varying from 30 to 1600 m, or closer distances if the limits are adjusted in inverse proportion to distance.

The CISPR specifies vertically and horizontally polarized E-field measurements at a fixed height of 3 m for Group 2 Class A equipment, and may be interpreted to require a 1–4 m height scan *in situ* for Group 1 and Group 2 Class B equipment. The FCC specifies height scans of 1–4 m at distances up to 10 m, and 2–6 m at distances greater than 10 m.

By their nature, ISM machines, generating RF powers up to 1 MW or more [3], can radiate high levels of spurious electromagnetic disturbances. To protect aeronautical services, it is important to know whether or not the specified *in situ* measurements accurately predict the field strengths created at elevated angles. Therefore, some

Manuscript received October 2, 1995; revised April 23, 1996.
The author is a consultant with EMC, Victoria 3134, Australia.
Publisher Item Identifier S 0018-9375(96)06145-5.

0018–9375/96$05.00 © 1996 IEEE